J. Chem. Sci. Vol. 128, No. 4, April 2016, pp. 621–631.
DOI 10.1007/s12039-016-1054-8

Interactions between metal cations with H_2 in the M^+- H_2 complexes: Performance of DFT and DFT-D methods

SRIMANTA PAKHIRA[a], TANAY DEBNATH[b], KAUSHIK SEN[b] and ABHIJIT K DAS[b,*]

[a]Graduate School of Information Science, Nagoya University, Chukusa-ku, Nagoya 464-8601, Aichi, Japan
[b]Department of Spectroscopy, Indian Association for the Cultivation of Science, Jadavpur, Kolkata 700 032, West Bengal, India
e-mail: srimantacu@yahoo.co.in; sptb2@iacs.res.in; kaushik.physichem@gmail.com; spakd@iacs.res.in

MS received 27 November 2015; revised 20 January 2016; accepted 26 January 2016

Abstract. The interactions between metal cations (Ni^+, Cu^+, Zn^+) and H_2 molecule have been investigated in detail using dispersion-corrected and -uncorrected double hybrid density functional (DHDF), gradient corrected density functional, ordinary density functional and CCSD(T) methods in conjunction with the correlation consistent triple-ζ quality basis sets. Structural properties, depth of the potential well and dissociation energies are calculated using DFT, DFT-D and CCSD(T) methods and are compared with experimental results. A comparative analysis has been made among DFT, DFT-D and CCSD(T) methods with respect to experiments. The energy components of the interaction energy have been estimated by the symmetry-adapted perturbation theory (SAPT) to analyze the effect of various components on the interaction of the complexes. The dispersion-corrected DHDF, mPW2PLYP-D method shows the best agreement with the experimental values. An NBO analysis has been performed to understand the orbital participation in metal ligand interaction and charge transfer process in these complexes.

Keywords. Interaction; metal cation–dihydrogen complexes; well depth; binding energy; PECs; energy components; DHDF; CCSD(T); SAPT; NBO.

1. Introduction

Interactions between metal cations and neutral molecules play important roles in a variety of contexts including gas storage in solid materials, ion solvation, laser plasmas, and atmospheric and astrophysical processes.[1,2] As H_2 burns completely free of pollutants,[3,4] it is the most efficient and cleanest fuel and can be considered as the best solution for the limited fossil fuel and the problem of climate change. It is thus considered as a sustainable energy carrier. Many studies have been conducted to draw attention to the storage of molecular hydrogen. Other important applications of the complexes formed by the interaction between metal cations and H_2 molecule can be found in guiding reactive molecular encounters occurring in the cold surroundings of interstellar space and in driving formation of stable non-covalent complexes in metal–organic frameworks (MOFs) and zeolites.[5] In a recent article[6] we have studied the interaction of metal cations (Mg^+, Ca^+, and Ag^+) with hydrogen molecule in order to understand how metal cations accumulate hydrogen. The objective of this article is two-fold, firstly, how accurately different DFT methods predict the structure and interaction of these complexes and secondly, how we can get in-depth understanding of the interaction and energy transfer between metal cation and dihydrogen through SAPT and NBO analysis.

Many theoretical and experimental techniques[7–12] have been devoted to study the metal cation-dihydrogen complexes to predict the structure, frequency, binding energy, and depth of the potential well, but the predicted theoretical results are much away from the available experimental values and in some cases the theoretical results are contradictory. Among various systems considered for this type of interaction, metal cation–dihydrogen (M^+–H_2, M = Metal) complexes are the charged polyatomic weakly bound complexes having binding energies typically less than 10 kcal/mol and are considered for assessing computational techniques aimed at studying ion-neutral complexes that are relevant for the hydrogen storage problem.[7] Kemper *et al.*,[8] studied the structure, frequencies, binding energies and depth of the potential well of Ni^+-H_2 systems using chromatography experiments, and they also performed a theoretical calculation at MP2 level to verify their experimental results. Kemper *et al.*,[9] and Manard *et al.*,[10] also carried out an experiment on the $Cu^+-(H_2)_n$ clusters using

*For correspondence

temperature dependent equilibrium measurement techniques to determine the binding energies and entropies of the complexes. The structures, geometries, vibrational frequencies, and origin of the bonding were also studied using density functional theory (DFT) and MP2 methods. Wies *et al*.,[11] performed a similar experiment on the $Zn^+-(H_2)_n$ clusters and reported the binding energy and entropy. The density functional theory was used to determine structure, frequency and orbital populations in support of their experimental data. Dryza and Bieske[12] recorded the infrared (IR) spectrum of Zn^+-D_2 and determined the structural and energetics parameters of $Zn^+-(H_2)$ complex from the spectroscopic data of Zn^+-D_2. But the reported theoretical results deviate much from the experimental values. To remove the discrepancy among the values reported by the earlier experimental and theoretical studies and in order to reproduce the experimental values, we have studied in detail the structural properties, interactions and various components of interaction energy of the metal cation–dihydrogen (M^+–H_2, M = Ni, Cu and Zn) complexes.

In this article, both the dispersion-corrected and–uncorrected double hybrid density functional (DHDF) and gradient corrected density functional (GGA) theories are used to study the metalcation–dihydrogen (M^+–H_2, where M = Ni, Cu and Zn) complexes. The charge of the Ni^+–H_2, Cu^+–H_2 and Zn^+–H_2 complexes are +1 and the multiplicity of these complexes are 2, 1 and 2, respectively. The coupled cluster CCSD(T)[13–15] method and symmetry adapted perturbation theory (SAPT)[16] have also been applied to verify the consistency of the values obtained by the dispersion-corrected DHDF theories. The SAPT analysis is performed to study the effects of various energy components on the interaction in these complexes. A comparative analysis has been made among the results obtained by DFT methods, dispersion-corrected and –uncorrected double hybrid density functional methods, CCSD(T) method and SAPT. An NBO analysis has been performed to fathom the interaction between the metal cations and hydrogen molecule.

2. Computational details

Recently, Grimme[17,18] proposed dispersion-corrected formalisms for both gradient-corrected and double hybrid density functional theories (DFT-D). These methods essentially improve the earlier methods[19,20] and are very useful for general chemistry applications. In this method,[17] the vdW dispersion correction is described by a damped interatomic R^{-6} potential. For larger complexes, Grimme demonstrated that the basis set superposition error (BSSE) could be avoided by using the DFT-D method in conjunction with triple-ζ quality basis sets.[17,20,21] For small complexes, as DHDFs include an MP2 part, which is sensitive to BSSE, the BSSE correction has been incorporated only at mPW-2PLYP-Dlevel. Therefore, BSSE has been computed both at mPW2PLYP-D and CCSD(T) levels. The extension '-D' stands for the long-range dispersion-corrected functionals(-D2) containing the interaction term.

Zaho *et al*.,[22] developed a doubly hybrid meta DFT, which generalizes the multi-coefficient methods to allow mixing of the wave function based methods with hybrid density functional methods. Grimme and co-workers[23,24] developed two new DHDFs, B2PLYP[23] and mPW2PLYP[24] and added dispersion correction to them that are able to treat long range and medium range dispersion effects effectively.[25] The DHDF methods without and with dispersion correction used in this calculation are B2PLYP,[23] mPW2PLYP[24,26] and B2PLYP-D, mPW2PLYP-D. To make a comparison among various DFT and *ab initio* methods for the structure, equilibrium distance, frequencies, frequency shift, PECs, depth of the potential well and dissociation energy of the systems (M^+–H_2, where M = Ni, Cu and Zn),we have employed the ordinary DFT and gradient corrected functional of Perdew–Bruke–Ernzerhof (PBE),[27] and their dispersion corrected formalisms, namely BLYP,[28,29] PBE and PBE-D, BLYP-D methods, along with the DHDFs (B2PLYP and mPW2PLYP) with and without dispersion correction and the CCSD(T)[13–15] method. The coupled cluster CCSD(T) method has also been applied to study geometrical parameters, depth of the potential well and ZPE-corrected dissociation energy of the metal cation–dihydrogen (M^+–H_2) complexes.

The double hybrid density functionals, B2PLYP and mPW2PLYP, described recently by Grimme and co-workers are based on the mixing of standard generalized gradient approximation with Hartree-Fock exchange and second order Møller-Plesset type correction, which comes from the Kohn-Sham (KS) orbitals and eigenvalues to calculate the exchange and correlation energy of the non-interacting system. Becke 88 (B88) exchange and Lee-Yang-Parr (LYP) correlation term are considered for B2PLYP, but only the exchange term is swapped by the modified Perdew-Wang (mPW) functional of Adamo and Barone[26] in the mPW2PLYP method.

All the DHDFs provide good results with minimum error compared to other hybrid and GGA functionals for several systems but they lack the description of dispersion forces. Although dispersion correction was

previously included into HF and DFT levels of theory by several groups,[30–32] in the present study we have applied the methodology of Grimme (to GGA functionals) where the van der Waals (vdW) interaction term is well explained by a damped interatomic potential.[23,24] The interaction potential takes into account the long-range dispersion effects in non-bonded systems. The total density functional energy can be written as

$$E_{DFT-D} = E_{DFT} + E_{vdW} \tag{1}$$

where E_{DFT} is the ordinary self-consistent density functional energy and E_{vdW} is the empirical dispersion corrected energy part (-D2), which is written as

$$E_{vdW} = -s_6 \sum_{i=1}^{N-1} \sum_{j=i+1}^{N} \frac{C_6^{ij}}{R_{ij}^6} f_{dmp}(R_{ij}) \tag{2}$$

In the above equation, s_6 is a scaling factor that depends entirely on the density functional and semi-empirical method. For the PBE, BLYP,B2LYP and mPW2PLYP functionals, Grimme determined the scaling factor by least-squares optimization of the deviations observed in the interaction energy values for the various weakly interacting systems.[18,25] The combined dispersion coefficient for the pair of atoms i and j (calculated from the atomic C_6 coefficients) is denoted by C_6^{ij}. R_{ij} is the interatomic distance between atoms i and j, $f_{\mathrm{dmp}}(R_{ij})$ is the damping function, and N is the number of atoms present in the system. The mathematical expression of the damping function, $f_{\mathrm{dmp}}(R_{ij})$, is as follows:

$$f_{dmp}(R_{ij}) = \frac{1}{1 + \exp\left\{-\beta\left(\frac{R}{R_0} - 1\right)\right\}} \tag{3}$$

Where β is taken to be 20 in the exponent.[18] This value of β gives larger corrections at intermediate distances.

The PECs are drawn using PBE, BLYP, B2PLYP and mPW2PLYP with and without long range dispersion corrected DHDF and CCSD(T) methods using the correlation consistent polarization valence triple-ζ quality basis sets (cc-pVTZ)[33,34] for all the atoms in the weakly bound metal cation–dihydrogen (M^+–H_2, where M = Ni, Cu and Zn) complexes. The spin-unrestricted methods are used for the Ni^+–H_2 and Zn^+–H_2 complexes as their multiplicity is two, and spin-restricted methods are used only for the Cu^+–H_2 complex as its multiplicity is one. The geometries of the complexes are optimized by all these methods using Gaussian 09 suite of quantum chemistry programs.[35] All other electronic structure calculations are performed using the ORCA[36] suite programs and the optimized electronic structures are visualized with ChemCraft.[37] The cation M^+(Ni^+, Cu^+ and Zn^+) is placed perpendicular to the molecular axis of H_2 and the distance between the cation and the center of mass of H_2 is denoted by R_e, *i.e.*, a perfect T-shaped geometry. The scanning of the interaction energy is then performed by varying the distance, R, between M^+ and center of mass of H_2 molecule, and calculating the single point energies at each R value without disturbing the perfect T-shaped geometry of the complexes. As stated earlier, Grimme[17,20,21] proved that, using the DFT-D method and zeta quality basis sets, much of the BSSE calculation is avoided,[38–40] which is otherwise essential for highly correlated methods like MP2 and CCSD(T). In fact the BSSE is absorbed into the empirical potential.[17,20,21] As the DFT-D methods with triple-ζ quality basis sets do not require BSSE correction,[38–40] the BSSE correction has been estimated only at CCSD(T)/cc-pVTZ level using the counterpoise methods of Boys and Bernardi.[41] To check the BSSE correction of the DFT-D method, we have calculated the BSSE corrected energy of these complexes only at mPW2PLYP-D method. Our computations show that the BSSE energy computed at mPW2PLYP-D level of theory is negligible. To calculate the BSSE correction energy, we have considered two natural fragments: M^+ (where $M^+ = Ni^+$, Cu^+ and Zn^+) and H_2. The BSSE correction for the Ni^+-H_2, Cu^+-H_2 and Zn^+-H_2 complexes are 0.798, 0.839 and 0.152 kcal/mol, respectively. The BSSE calculations at CCSD(T)/cc-pVTZ level of theory are performed with the optimized geometries of these complexes.

In order to estimate the dispersion and other effects on the complexes, we have applied SAPT to calculate different terms contributing to the interaction energy. These are electrostatic, polarization, dispersion, exchange, and repulsion energy terms. The SAPT calculations are performed with cc-pVTZ basis set using the GAMESS[42–44] electronic structure codes interfacing the SAPT2008.1 program[45] for the Cu^+-H_2 complex and open-shell SAPT (DFT) 2008 program[46] for the Ni^+-H_2 and Zn^+-H_2 complexes. The mPW2PLYP method is used to calculate SAPT(DFT). An NBO analysis, as implemented in Gaussian 09,[35] has been performed with the optimized geometries of these complexes.

3. Results and Discussion

The optimized geometry of the metal cation–dihydrogen (M^+–H_2, where M = Ni, Cu and Zn) complexes is depicted in figure 1 along with their geometrical parameters. Only T-shaped isomers of these complexes are described here because the T-shaped isomers are more stable than the linear isomers. Although the symmetry

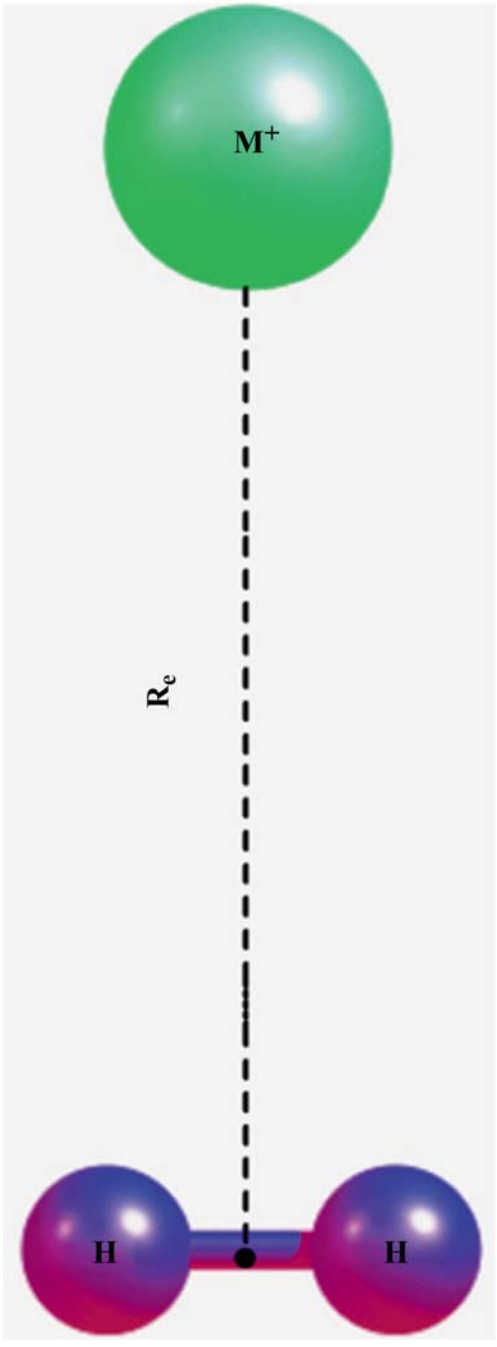

Figure 1. Geometrical configuration and parameters of the metal cation-dihydrogen (M^+–H_2; M = Ni, Cu and Zn) complexes. The dotted line presents the equilibrium bond distance, R_e, between the cation and center of mass of H_2 molecule.

of the isomers is C_{2v}, the results remain unchanged in their reduced symmetry, C_1.

The geometrical parameters for the Ni^+–H_2, Cu^+–H_2, and Zn^+–H_2 metal cation–dihydrogen complexes are summarized in table 1 along with theoretical and experimental values.

The experimental values are available only for Zn^+–H_2 complex. It is observed from the table that for all the complexes the equilibrium R_e distance, r_{HH} bond distance and bond shift Δr_{HH} calculated by the dispersion-corrected mPW2PLYP-D method are almost same as those calculated by CCSD(T) method. It may be noted that the equilibrium R_e distance calculated by PBE and BLYP methods is lower than that obtained by mPW2-PLYP and CCSD(T) methods. Also, both dispersion-corrected and –uncorrected methods give almost same values for these geometrical parameters. It appears that dispersion has negligible effect on the geometrical parameters. For the first two complexes, the results obtained by B2PLYP and mPW2PLYP methods are consistent with the reported theoretical and experimental values, and for the Zn^+–H_2 complex, the mPW2PLYP-D values agree very well with the experimental values. Among the three complexes, Δr_{HH} (it is the difference between the bond length of H_2 in the complexes and the bond length of free H_2) value is same for the Ni^+-H_2 and Cu^+-H_2 complexes and this value is greater than that of the Zn^+-H_2 complex. The large Δr_{HH} may be due to the greater electron delocalization of the H-H bond towards the Ni^+ and Cu^+ cations than the Zn^+ cation, which makes the H-H bond weak.

The harmonic vibrational frequencies of the complexes are displayed in table 2. The reported values are mostly theoretical, and the experimental results are available only for the Zn^+-H_2 complex. In general, the frequencies ν_1 and ν_2 decrease but the frequency ν_3 increases with improvement of functional. Among the five methods, mPW2PLYP-D method provides the best results. For Ni^+-H_2 complex, the stretching frequency, ν_1, between the center of mass of the H_2 molecule and Ni^+ cation, and the asymmetric bending frequency, ν_2, obtained at mPW2PLYP-D level are smaller than the reported theoretical values of Kemper *et al*.,[8] who used 'SVP' basis set for hydrogen and 'ECP-10-MDF' for nickel, which are smaller basis sets for this complex. The free stretching frequency, ν_3, between the H atoms of the complex, and the frequency shift $\Delta\nu_3$ (it is the difference between the frequency of H_2 in the complexes and the frequency of free H_2) are consistent with the reported theoretical values. For the Cu^+-H_2 complex, three vibrational frequencies and shift calculated by mPW2PLYP-D method are in good agreement with the earlier theoretical values of Kemper *et al*.[9] It may be noted that for these two complexes the vibrational frequencies and frequency shift calculated by mPW2PLYP and mPW2PLYP-D methods are almost same and dispersion has no effect on the vibrational frequencies. For the Zn^+-H_2 complex, the dispersion effect generally reduces the vibrational frequencies. The stretching frequency, ν_1, computed at mPW2PLYP-D level is about 15 cm^{-1} lower than the experimental value of Dryza and

Table 1. Geometrical parameters for the M^+–H_2 (M: Ni, Cu and Zn) weakly bound complexes at different theoretical levels.

		Parameters			
Methods	Complexes	R_e (Å)	r_{HH}(Å)	Δr_{HH}(Å)	r'_{HH}(Å) [H-H]
PBE		1.59	0.83	0.08	0.75
PBE-D		1.59	0.83	0.08	0.75
BLYP		1.63	0.81	0.06	0.75
BLYP-D	Ni^+-H_2	1.63	0.81	0.06	0.75
B2PLYP		1.67	0.79	0.05	0.74
B2PLYP-D		1.67	0.79	0.05	0.74
mPW2PLYP		1.68	0.78	0.04	0.74
mPW2PLYP-D		1.68	0.78	0.04	0.74
CCSD(T)		1.69	0.78	0.03	0.75
Experiment					0.74[e]
Theory		1.65[a]	0.79[a]	0.06[a]	0.74[f]
PBE		1.63	0.82	0.07	0.75
PBE-D		1.65	0.81	0.06	0.75
BLYP		1.66	0.80	0.05	0.75
BLYP-D	Cu^+-H_2	1.65	0.81	0.06	0.75
B2PLYP		1.69	0.78	0.04	0.74
B2PLYP-D		1.69	0.78	0.04	0.74
mPW2PLYP		1.70	0.78	0.04	0.74
mPW2PLYP-D		1.70	0.78	0.04	0.74
CCSD(T)		1.72	0.78	0.03	0.75
Experiment					0.74[e]
Theory		1.70[b]	0.78[b]	0.04[b]*	0.74[f]
PBE		2.20	0.78	0.03	0.75
PBE-D		2.24	0.79	0.04	0.75
BLYP		2.27	0.76	0.01	0.75
BLYP-D	Zn^+-H_2	2.20	0.77	0.02	0.75
B2PLYP		2.28	0.75	0.01	0.74
B2PLYP-D		2.35	0.75	0.01	0.74
mPW2PLYP		2.28	0.75	0.01	0.74
mPW2PLYP-D		2.32	0.75	0.01	0.74
CCSD(T)		2.32	0.76	0.01	0.75
Experiment		2.32[c]	0.76[c]	0.02[c]*	0.74[e]
Theory		2.25[d]	0.77[d]	0.03[d]*	0.74[f]

[a]Ref. [8], [b]Ref. [9], [c]Ref. [12], [d]Ref. [11], [e]Ref. [47], [f]Ref. [46] *Calculated from available value.

Bieske[12] and the frequency shift agrees within 5 cm^{-1} with the experimental value. The CCSD(T) and earlier theoretical results are much away from the experiment. The results obtained by PBE and BLYP methods deviate much from the experimental values.

The PECs of the T-shaped isomers of the metal cation–dihydrogen complexes are depicted in figures 2, 3 and 4, respectively. The PECs are drawn with the relative interaction energies between the respective cations and hydrogen molecule versus the distance, R, between the cations and center of mass of H_2 molecule.

The results from the PECs calculated at different levels of theory are collected in table 3. The equilibrium distance (R_e) of the Ni^+–H_2 complex calculated at BLYP, B2PLYP and mPW2PLYP levels is consistent with the reported value of Kemper *et al*.[8] Both mPW2PLYP and CCSD(T) methods give the same value. The depth of the potential well, D_e, of this complex at mPW2PLYP-D level is in very good agreement with the experimental value of Kemper *et al*.[8]

The bond dissociation energy, D_o, of this complex at mPW2PLYP-D level also reproduces the experimental value. The values of D_e and D_o of the Ni^+–H_2 complex obtained at CCSD(T) method are about 16.37 and 14.27 kcal/mol, respectively, which are little lower than the experimental values of Kemper *et al*.[8] The other three methods, namely PBE, BLYP and B2PLYP overestimate D_e and D_0. The well depth and dissociation

Table 2. Comparison of frequencies and stretching frequency shifts with the available experimental and theoretical values for the M^+–H_2 (M: Ni, Cu and Zn) complexes.

		Parameters			
Methods	Complexes	ν_1 (cm^{-1})	ν_2 (cm^{-1})	ν_3(cm^{-1})	$\Delta\nu_3$(cm^{-1})
PBE		972.7	1475.8	3174.3	1157.4
PBE-D		965.8	1474.6	3171.7	1159.9
BLYP		972.1	1362.2	3361.3	1000.4
BLYP-D		925.4	1369.2	3366.1	995.5
B2PLYP	Ni^+–H_2	877.1	1308.9	3756.4	713.6
B2PLYP-D		875.9	1308.1	3756.3	713.7
mPW2PLYP		872.9	1290.1	3809.4	670.6
mPW2PLYP-D		871.6	1288.7	3810.2	669.8
CCSD(T)		808.1	1233.2	3823.2	586.8
Theory		874[a]	1378[a]	3835[a]	574[a]*
PBE		967.7	1281.9	3440.4	891.3
PBE-D		966.2	1281.0	3439.9	891.7
BLYP		895.6	1193.2	3557.2	804.5
BLYP-D		907.0	1198.2	3553.6	808.0
B2PLYP	Cu^+–H_2	855.0	1170.1	3848.8	621.2
B2PLYP-D		852.4	1168.7	3849.4	620.3
mPW2PLYP		846.8	1155.7	3886.6	593.4
mPW2PLYP-D		844.7	1154.0	3886.9	593.1
CCSD(T)		775.4	1091.1	3909.1	500.9
Theory		881[b]	1146[b]	3772[b]	637[b]*
PBE		399.4	440.2	4040.4	291.3
PBE-D		339.8	361.5	4045.7	291.2
BLYP		346.4	367.9	4085.2	276.5
BLYP-D		299.0	323.5	4108.8	252.8
B2PLYP	Zn^+–H_2	352.3	478.8	4249.3	220.7
B2PLYP-D		313.4	461.9	4259.7	210.3
mPW2PLYP		353.6	483.1	4259.8	220.2
mPW2PLYP-D		324.6	472.4	4265.6	214.4
CCSD(T)		306.7	506.0	4232.0	178.0
Expt.		340[c]			219[c]
Theory		394[c], 482[d]	427[c], 498[d]	4172[d]	235[c], 184[d]*

[a] Ref. [8], [b]Ref. [9], [c]Ref. [12], [d]Ref. [11], [e]Ref. [47], [f]Ref. [46] *Calculated from available value.

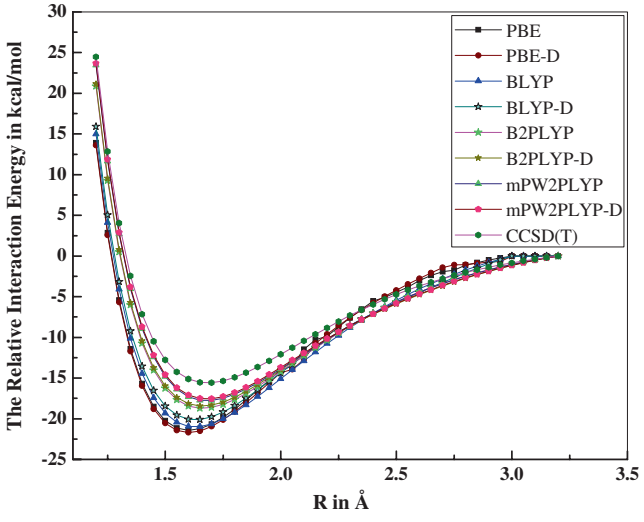

Figure 2. Potential energy curves (PECs) at different methods (PBE, BLYP, B2PLYP, mPW2PLYP, PBE-D, BLYP-D, B2PLYP-D, mPW2PLYP-D, and CCSD(T)) for the T-shaped Ni^+–H_2 complex. *R* is the separation between Ni^+ cation and the center of mass of H_2 molecule.

energy of the Cu^+–H_2 complex at mPW2PLYP-D level are very close to the experimental values of Kemper *et al.*[9] The results obtained by BLYP and B2PLYPmethods are also consistent with the experimental values, whereas the PBE method overestimates both D_e and D_0. The CCSD(T) values for the depth of the potential well (13.36 kcal/mol) and dissociation energy (11.26 kcal/mol) of the Cu^+–H_2 complex are lower than the experimental values of Kemper *et al.*[9] The earlier theoretical results are also away from the experimental values. The equilibrium distance, R_e, calculated at mPW2PLYP-D level is same as the reported theoretical value. Situation is little different for the Zn^+-H_2 complex. The bond dissociation energy (D_o) and well depth (D_e) of the Zn^+-H_2 complex computed by PBE-D and BLYP-D methods are consistent with the experimental values of Wies *et al.*,[11] and Dryza and Bieske.[12] However, the best agreement with the experimental values is obtained for the mPW2PLYP-D method. The CCSD(T) values for D_e and D_o of the

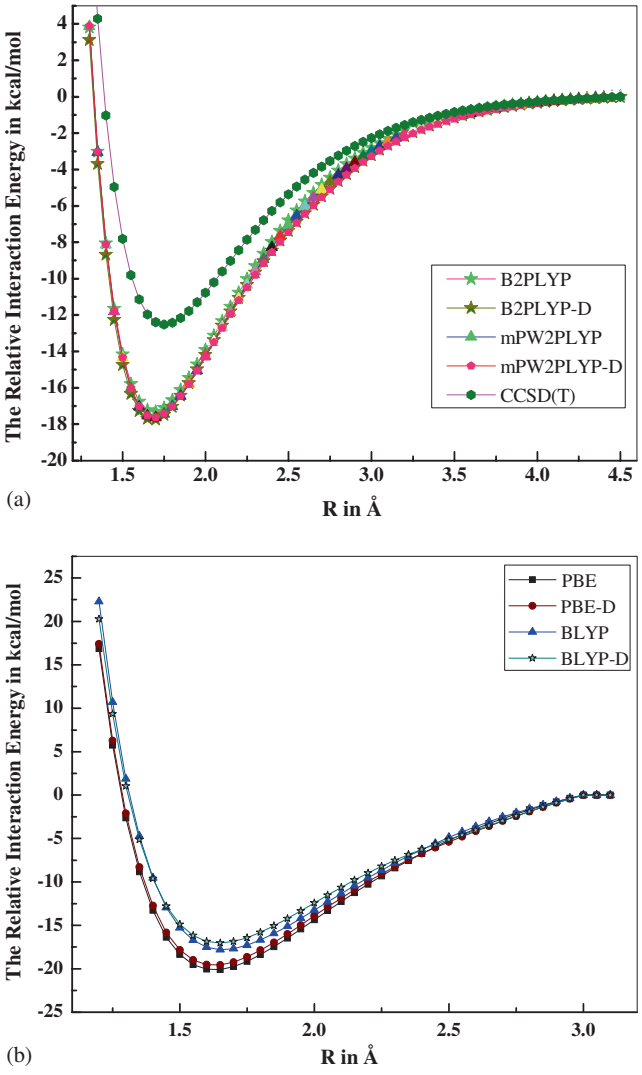

Figure 3. Potential energy curves (PECs) for the T-shaped Cu^+–H_2 complex at **(a)** B2PLYP, mPW2PLYP, B2PLYP-D, mPW2PLYP-D, and CCSD(T) methods and **(b)** PBE, BLYP, PBE-D and BLYPD methods. *R* is the separation between Cu^+ cation and the center of mass of H_2 molecule.

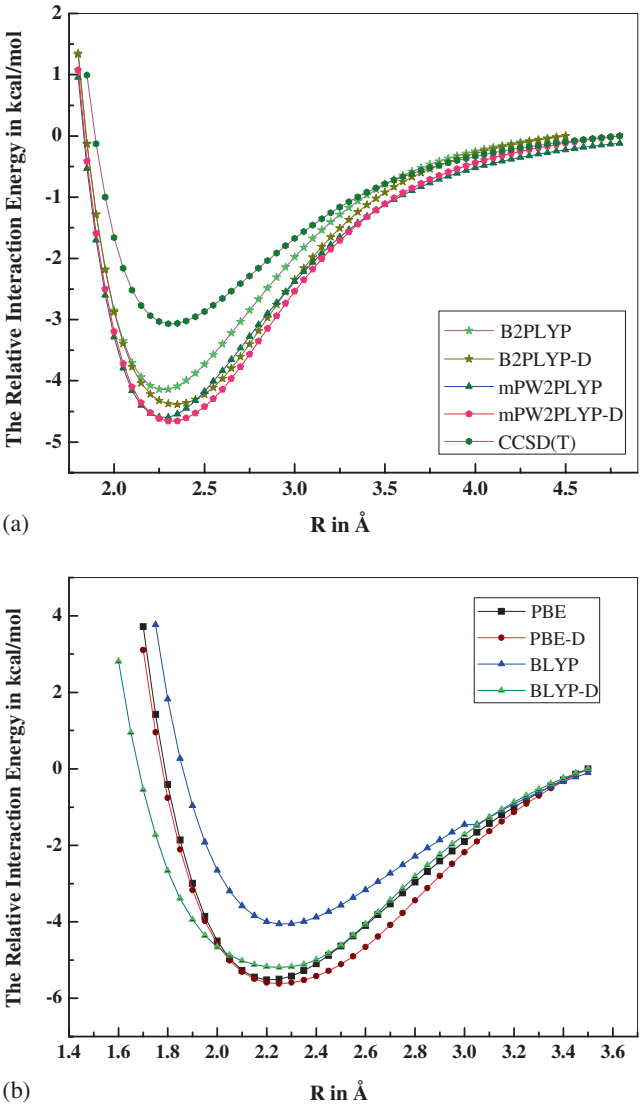

Figure 4. Potential energy curves (PECs) for the T-shaped Zn^+–H_2 complex at **(a)** B2PLYP, mPW2PLYP, B2PLYP-D, mPW2PLYP-D, and CCSD(T) methods and **(b)** PBE, BLYP, PBE-D and BLYPD methods. *R* is the separation between Zn^+ cation and the center of mass of H_2 molecule.

Zn^+–H_2 complex are about 3.22 and 2.31 kcal/mol; these values are also lower than the experimental values.[11,12] It is important to note that the bond dissociation energy and depth of the well for both Ni^+–H_2 and Cu^+–H_2 complexes are almost same and these values are much greater than those of the Zn^+−H_2 complex. Therefore, the interaction between the metal cations and H_2 in Ni^+–H_2 and Cu^+–H_2 complexes is much stronger than that in the Zn^+−H_2 complex.

The total SAPT interaction energies and the contributing components for all the metal cation–dihydrogen complexes are collected in table 4. The SAPT is based on the many-body perturbation theory and it provides relative energies that are as accurate as correlated methods. The results of well depth and dissociation energy obtained by the mPW2PLYP-D and CCSD(T) methods are also given in the table for comparisons.

The total SAPT interaction energies, E_{int} (SAPT Total), are in good agreement with the well depths calculated by mPW2PLYP-D method; deviation varies from 0.54 to 2.06 kcal/mol. The terms that contribute to the vdW interaction are electrostatic, polarization, dispersion and exchange. The sum of the electrostatic, dispersion, polarization and exchange terms is denoted by "total attraction" and the repulsion term is denoted by "total repulsion". The algebraic sum of "total attraction" and "total repulsion" is the total SAPT interaction energy, E_{int} (SAPT Total). In the Ni^+–H_2 complex, the electrostatic, polarization, and exchange dominate

Table 3. Depth of the potential well (D_e in kcal/mol), dissociation energy (D_o in kcal/mol) and equilibrium distances (R_e & r_{HH} in Å) from the PECs at different theoretical levels for the M^+–H_2 (M: Ni, Cu and Zn) complexes and comparison with earlier experimental and theoretical values.

Methods	Complexes	Parameters				
		R_e	r_{HH}	D_e	ΔZPE	D_o
PBE		1.60	0.83	19.66	1.85	18.81
PBE-D		1.60	0.83	21.71	1.83	19.88
BLYP		1.65	0.81	20.97	1.84	19.13
BLYP-D	Ni^+-H_2	1.65	0.81	20.01	1.85	18.16
B2PLYP		1.65	0.79	18.71	2.25	16.46
B2PLYP-D		1.65	0.79	18.44	2.25	16.79
mPW2PLYP		1.70	0.78	17.75	2.15	15.4
mPW2PLYP-D		1.70	0.78	17.77	2.14	15.63
CCSD(T)		1.70	0.78	16.37	2.1	14.27
Experiment				17.3 ± 0.3[a]		15.15 ± 0.3[a*]
Theory		1.654[a]	0.79[a]	17.90[a]		15.60[a]
PBE		1.65	0.82	20.80	1.94	18.86
PBE-D		1.65	0.81	19.55	1.95	17.6
BLYP		1.65	0.80	17.79	1.83	15.96
BLYP-D	Cu^+-H_2	1.65	0.81	17.04	1.85	15.19
B2PLYP		1.70	0.78	17.31	2.15	15.16
B2PLYP-D		1.70	0.78	17.73	2.15	15.58
mPW2PLYP		1.70	0.78	17.63	2.03	15.6
mPW2PLYP-D		1.70	0.78	17.88	2.02	15.86
CCSD(T)		1.75	0.78	13.36	2.1	11.26
Experiment				17.4 ± 1.0[b*]		15.4 ± 1.0[b]
Theory		1.70[b]	0.78[b]	18.1[b], 18.6[b]		16.2[b], 16.6[b]
PBE		2.20	0.78	4.51	0.79	3.72
PBE-D		2.25	0.79	4.48	0.60	3.88
BLYP		2.20	0.76	4.06	0.62	3.44
BLYP-D	Zn^+-H_2	2.25	0.77	3.92	0.52	3.40
B2PLYP		2.25	0.75	4.14	1.02	3.12
B2PLYP-D		2.35	0.75	4.38	0.96	3.42
mPW2PLYP		2.30	0.75	4.60	0.89	3.71
mPW2PLYP-D		2.25	0.75	4.73	0.85	3.88
CCSD(T)		2.30	0.76	3.22	0.91	2.31
Expt.		2.32[c]	0.76[c]	4.6 ± 0.4[d*]		3.75 ± 0.4[d], 3.745[c]
Theory		2.25[c], 2.27[d]	0.77[d]	6.06[d]		4.94[d], 4.57[c]

[a] Ref. [8], [b]Ref. [9], [c]Ref. [12], [d]Ref. [11] *Calculated from available value.

over the dispersion component in the attraction term. The energy components decrease from the Ni^+–H_2 to the Zn^+-H_2 complex, with a sharp decrease from Cu^+-H_2 to Ni^+-H_2 complex. In Zn^+-H_2 complex, the exchange term is the main contributor to the attraction energy compared to electrostatic, polarization and dispersion components which have comparable contributions. The energy components are plotted against the complexes in figure 5.

It is observed from figure 5, that the electrostatic component of Cu^+-H_2 is about four times as that of Zn^+-H_2, and the polarization component decreases about half from $Ni^+-H_2$to Cu^+-H_2 and then from Cu^+-H_2 to Zn^+-H_2 complex. The dispersion components of Ni^+–H_2 and Cu^+-H_2 are almost same but it decreases sharply from Cu^+-H_2 to Zn^+-H_2 complex. In contrast, the exchange component first increases from Ni^+-H_2 to Cu^+-H_2 and then from Cu^+-H_2 to Zn^+-H_2 complex. The total attraction and repulsion energies are highest for the Ni^+-H_2 complex. The interaction energy, E_{int}, which is nothing but the depth of the potential well, calculated by SAPT for all the complexes is very close to that calculated at mPW2PLYP-D/cc-pVTZ level. It may be noted that well depths or interaction energies calculated by SAPT for the Ni^+-H_2 and Cu^+-H_2 complexes differs by 2.87 kcal/mol, whereas those obtained by mPW2PLYP-D/cc-pVTZ method are almost same, which is supported by

Table 4. SAPT/cc-pVTZ interaction energy components (kcal/mol) for M^+–H_2 (M: Ni, Cu and Zn) complexes.

Energy Components (SAPT)	Systems		
	Ni^+-H_2	Cu^+-H_2	Zn^+-H_2
Electrostatic	−29.23	−25.13	−5.95
Polarization	−37.97	−15.05	−8.16
Dispersion	−12.30	−11.44	−3.29
Exchange	−21.50	−32.08	−14.96
Repulsionenergy	82.31	67.88	28.17
Total attraction	−101.00	−83.70	−32.36
Total repulsion	82.31	67.88	28.17
E_{int} (SAPT)	−18.69	−15.82	−4.19
$^{\dagger}D_e$ (SAPT)	18.69	15.82	4.19
D_0 (SAPT)	16.54	13.08	3.29
CCSD(T)/cc-pVTZ			
D_e	16.37	13.36	3.22
D_o	14.27	11.26	2.31
mPW2PLYP-D/cc-pVTZ			
D_e	17.77	17.88	4.73
D_o	15.63	15.86	3.73
Experimental results			
D_e	17.3 ± 0.3^a	$17.4 \pm 1.0^{b*}$	$4.6 \pm 0.4^{c*}$
D_o	$15.15 \pm 0.3^{a*}$	15.4 ± 1.0^b	3.75 ± 0.4^c

[a]Ref. [8], [b]Ref. [9], [c]Ref. [11]; *Calculated from available value; $^{\dagger}D_e$ (SAPT) = $|E_{int}$ (SAPT)|

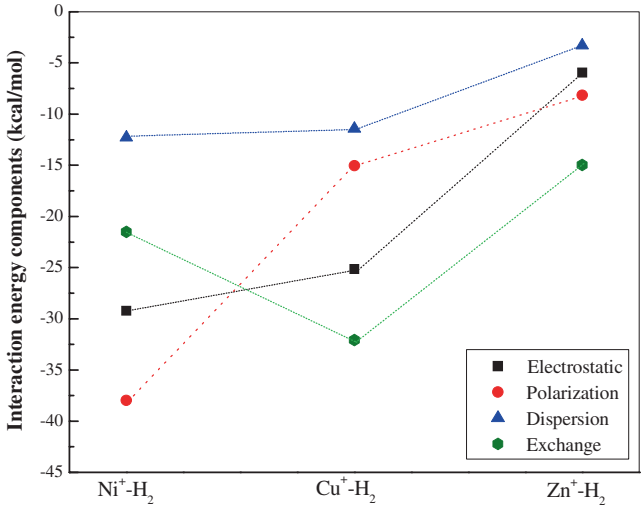

Figure 5. Interaction energy components *vs* metal cation-dihydrogen M^+–H_2 (M =Ni, Cu and Zn) complexes.

the experimental results of Kemper *et al.*[8,9] The interaction energy, E_{int}, of the Zn^+-H_2 complex is lowest among the three complexes and it is also consistent with our calculated value at mPW2PLYP-D level as well as earlier experimental values of Weis *et al.*[11]

Analyzing the energy components, we have observed that electrostatic, polarization and dispersion energy decrease from Ni^+ to Cu^+ and fall sharply for Zn^+. Same trend is also observed in case of repulsion energy. From natural bonding orbital (NBO) analysis, summarized in table 5, we have found that in Ni^+ occupancy of 4s orbital is almost negligible and 3d orbitals are also not fulfilled. In case of Cu^+, s occupancy is also negligible but greater than Ni^+. The 4s orbital of Zn^+ is half filled, much greater s occupancy than Ni^+ and Cu^+. Thus, it is evident that electrostatic, polarization and dispersion energies increase with increase of s occupancy. As the attraction energy decreases, the distance between the metal cation and dihydrogen increases from Ni^+-H_2 to Zn^+-H_2. This is also reflected in repulsion energy as it decreases from Ni^+-H_2 to Zn^+-H_2. Therefore, it is concluded that attraction and repulsion are dictated by s occupancy; more the occupancy less the attraction energy, lesser the attraction energy greater is the distance between the metal cation and dihydrogen, and finally greater is the distance lesser the repulsion energy. It is also observed that the energy transfer phenomenon depends on the valence *s* occupancy of the metal cation, as energy transfer from dihydrogen to metal cation decreases from Ni^+ to Zn^+. Therefore, from NBO analysis it can be inferred that vacancy of the valence orbital plays an important role in controlling

Table 5. Valence s orbital occupancy and energy transfer in M^+–H_2 (M: Ni, Cu and Zn) complexes.

Metal Cation (M^+)	Valence s (4s) orbital Occupancy	M^+-H_2 distance (Å)	Energy transfer to dihydrogen (kcal/mol)
Ni^+	0.03	1.7	20.2
Cu^+	0.05	1.7	18.9
Zn^+	1.02	2.3	8.8

all the energy components (both attraction and repulsion) including the energy transfer from ligand to metal cation.

4. Conclusions

Structures, frequencies, binding energy, depth of the potential well, potential energy PECs and various components of interaction between the metal cations (Ni^+, Cu^+ and Zn^+) and hydrogen molecule of the Ni^+-H_2, Cu^+-H_2 and Zn^+-H_2 complexes are studied in detail using the dispersion corrected and uncorrected density functional, CCSD(T) and SAPT methods. Among all the methods, the dispersion corrected mPW2PLYP-D method gives the best results which agree very well with the earlier experimental values. SAPT calculation has been performed to analyze the contributions of various energy components to the interaction energy. Among three complexes, the Ni^+-H_2 and Cu^+-H_2 complexes are more stable than Zn^+-H_2, as their dissociation energies as well as depth of the potential wells are the greatest. The Zn^+–H_2 complex is the least stable as the interaction between Zn^+ and H_2 is the lowest and also its dissociation energy is lowest among the three complexes. The SAPT calculation shows that in Ni^+-H_2 complex polarization, electrostatic and exchange dominate over the dispersion component, and in Cu^+-H_2 exchange, electrostatic and polarization contribute mainly to the attraction energy. In Zn^+-H_2 complex, sum of polarization, electrostatic and dispersion is almost same as exchange component in the attraction energy which is close to the repulsion energy. The NBO analysis establishes that vacancy of the valence orbitals regulates all the energy components (both attraction and repulsion) including the energy transfer from ligand to metal cation.

Acknowledgements

Srimanta Pakhira thanks Japan Society for the Promotion of Science (JSPS) for supporting his Post-Doctoral Research Fellowship for Foreign Researchers. A.K. Das is grateful to the Council of Scientific and Industrial Research (CSIR), Government of India, for a research grant under scheme number: 03(1168)/10/EMR-II. Kaushik Sen and Tanay Debnath are grateful to the Council of Scientific and Industrial Research (CSIR), Government of India, for providing research fellowships.

References

1. Dryza V, Poad B L J and Bieske E J 2012 *Phys. Chem. Chem. Phys.* **14** 14954
2. Lamsabhi A M, Mó O, Yáñez M, Guillemin J, Haldys V, Tortajada J and Salpin J 2008 *J. Mass Spect.* **43** 317
3. Panella B 2006 Ph.D. Thesis (Universität Stuttgart)
4. Schüth F 2006 *Nachr. Chem.* **54** 24
5. Nagaoka M, Ohta Y and Hitomi H 2007 *Coord. Chem. Rev.* **251** 2522
6. Sen K, Pakhira S, Sahu C and Das A K 2014 *Mol. Phys.* **112** 182
7. Dryza V and Bieske E J 2011 *J. Phys. Chem. Lett.* **2** 719
8. Kemper P R, Weis P and Bowers M T 1998 *Chem. Phys. Lett.* **293** 503
9. Kemper P R, Weis P, Bowers M T and Maitre P 1998 *J. Am. Chem. Soc.* **120** 13494
10. Manard M J, Bushnell J E, Bernstein S L and Bowers M T 2002 *J. Phys. Chem. A* **106** 10027
11. Weis P, Kemper P R and Bowers M T 1997 *J. Phys. Chem. A* **101** 2809
12. Dryza V and Bieske E 2009 *J. Chem. Phys.* **131** 224304
13. Kobayashi R and Rendell A P 1997 *Chem. Phys. Lett.* **265** 1
14. Cizek J and Paldus J 1971 *Int. J. Quant. Chem. Symp.* **5** 359
15. Purvis G D and Bartlett R J 1982 *J. Chem. Phys.* **76** 1910
16. Jeziorski B, Moszynski R and Szalewicz K 1994 *Chem. Rev.* **94** 1887
17. Grimme S 2004 *J. Comput. Chem.* **25** 1463
18. Grimme S 2006 *J. Comput. Chem.* **27** 1787
19. Elstner M, Hobza P, Frauenheim T, Suhai S and Kaxiras E 2001 *J. Chem. Phys.* **114** 5149
20. Wu X, Vargas M C, Nayak S, Lotrich V and Scoles G 2001 *J. Chem. Phys.* **115** 8748
21. Parac M, Etinski M, Peric M and Grimme S 2005 *J. Chem. Theo. Comput.* **1** 1110
22. Zhao Y, Lynch B J and Truhlar D G 2004 *J. Phys. Chem. A* **108** 4786
23. Grimme S 2006 *J. Chem. Phys.* **124** 034108
24. Schwabe T and Grimme S 2006 *Phys. Chem. Chem. Phys.* **8** 4398
25. Schwabe T and Grimme S 2007 *Phys. Chem. Chem. Phys.* **9** 3397

26. Adamo C and Barone V 1998 *J. Chem. Phys.* **108** 664
27. Perdew J P, Burke K and Ernzerhof M 1996 *Phys. Rev. Lett.* **77** 3865
28. Becke A D 1988 *Phys. Rev. A* **38** 3098
29. Lee Ch, Young W and Parr R G 1988 *Phys. Rev. B* **37** 785
30. Zimmerli U, Parrinello M and Koumoutsakos P 2004 *J. Chem. Phys.* **120** 2693
31. Douketis C, Scoles G, Marchetti S, Zen M and Thakkar A J 1982 *J. Chem. Phys.* **76** 3057
32. Merecero J M, Maxtrain J M, Lopez X, York D M, Largo A, Eriksson L A and Ugalde J M 2005 *Int. J. Mass Spectrom.* **240** 37
33. Dunning T H 1989 *J. Chem. Phys.* **90** 1007
34. Balabanov N B and Peterson K A 2005 *J. Chem. Phys.* **123** 064107
35. Frisch M J *et al.*, 2009, *Gaussian 09, Revision B.01* (Gaussian, Inc., Wallingford, CT)
36. Neese F 2010 *ORCA, version 2.80*, Institutfuer Physikalische und Theoretische Chemie, Universitaet Bonn, Germany
37. Zhurko G A and Zhurko D A *ChemCraft, Vers. 1.6* (**2010**)
38. Pakhira S, Sahu C, Sen K and Das A K 2012 *Chem. Phys. Lett.* **549** 6
39. Pakhira S, Sen K, Sahu C and Das A K 2013 *J. Chem. Phys.* **138** 164319
40. Seal P and Chakrabarti S 2009 *J. Phys. Chem. A* **113** 1377
41. Boys S F and Bernardi F 1970 *Mol. Phys.* **19** 553
42. Gordon M S and Schmidt M W 2005 *Theory and Applications of Computational Chemistry: The First Forty years* (Amsterdam: Elsevier)
43. Schmidt M W, Baldridge K K, Boatz J A, Elbert S T, Gordon M S, Jensen J H, Koseki S, Matsunaga N, Nguyen K A, Su S, Windus T L, Dupuis M and Montgomery Jr. J A 1993 *J. Comput. Chem.* **14** 1347
44. Bukowski R, Cencek RW, Jankowski P, Jeziorska M, Jeziorski B, Kucharski S A, Lotrich V F, Misquitta A J, Moszynski R, Patkowski *et al*. 2009, *SAPT2008.1*, University of Delaware and University of Warsaw, Newark
45. Żuchowski P S, Podeszwa R, Moszyński R, Jeziorski B and Szalewicz K 2008 *J. Chem. Phys.* **129** 084101
46. Jennings D E and Brault J W 1983 *J. Mol. Spectros.* **102** 265
47. Huber K P and Herzberg G 1979 *Molecular Spectra and Molecular Structure IV: Constants of Diatomic Molecules* (New York: Van Nostrand)